Acta Crystallographica Section B
Structural Science
ISSN 0108-7681

Influence of pressure on the lengths of chemical bonds

I. David Brown,* Peter Klages† and Aniceta Skowron‡

Brockhouse Institute for Materials Research, McMaster University, Hamilton, Ontario Canada L8S 4M1

† Current address: Department of Physics, Dalhousie University, Halifax, NS, Canada.
‡ Current address: Bodycote Materials Testing, s395 Speakman Drive, Mississauga, Ontario L5K 1B3, Canada

Correspondence e-mail: idbrown@mcmaster.ca

Received 19 December 2002
Accepted 12 May 2003

An expression to describe the force that a chemical bond exerts on its terminal atoms is proposed, and is used to derive expressions for the bond force constant and bond compressibility. The unknown parameter in this model, the effective charge on the atoms that form the bond, is determined by comparing the derived force constants with those obtained spectroscopically. The resultant bond compressibilities are shown to generally agree well with those determined from high-pressure structure determinations and from the bulk moduli of high-symmetry structures. Bond valences can be corrected for pressure by recognizing that the bond-valence parameter, R_0, changes with pressure according to the equation

$$\mathrm{d}R_0/\mathrm{d}P = 10^{-4}R_0^4/(1/B - 2/R_0)\ \text{Å GPa}^{-1}$$

1. Introduction

The purpose of this paper is to explore the influence of external pressure on the lengths of bonds found in inorganic crystals and to compare its effects with a classical force constant model. A full understanding of the response of a crystal to pressure must also take into account the effects of pressure on the soft van der Waals contacts since in many compounds the bulk modulus will be determined by these weaker interactions. Some of these van der Waals contacts determine the behaviour of the bonds themselves and to that extent they are implicitly included in the model, but otherwise they are beyond the scope of the present study. Their effect on the bulk modulus, even though it may be important, is not considered in this paper.

Because the development of a quantitative model based on the properties of chemical bonds requires a clear understanding of the underlying assumptions, and because these assumptions are often not discussed, we review them with some care in this first section of this paper. In §2 we develop a quantitative model for the force in a bond from which we derive expressions for the bond force constant and the bond compressibility. We compare the model with measurements in §3 where we show how to correct bond valences for pressure. We draw the threads together in §4.

1.1. Interaction between atoms: bonds and contacts

The assumption that the forces in a crystal act through localized bonds is not well supported by theory although it is often taken for granted. However, recently it has been shown to be valid in the ionic limit (Preiser *et al.*, 1999) and this demonstration has been extended to include bonds with

covalent character (Brown, 2001, p. 30). It is legitimate therefore to treat a crystal as an array of atoms in which only neighbouring atoms interact, that is, the only interactions that need to be considered are those between atoms that are linked by bond paths in the electron density topology[1] (Bader, 1990). These interactions can be divided into two classes: bonds, which involve shared valence electrons, and van der Waals contacts, which do not, the distinction being more carefully explained below. Both bonds and contacts contribute to the stabilization of the crystal although they differ considerably in strength.

It is readily shown that in the classical limit two spherical, rigid, electrically neutral atoms do not exert any force on each other when well separated, but as soon as their electron densities overlap the electrons in one atom will experience the electric field of the nucleus of the other and pull the two nuclei together. Atoms thus behave as if they are sticky; they exert no force on each other until they come into contact, at which point they attract each other. Since this result applies to all atoms without exception, all substances, even He, will condense into solids or liquids at sufficiently low temperatures. The attraction between the atoms increases as the overlap of the electron densities increases and, in the absence of the Fermi (*i.e.* Pauli) repulsion, would ultimately cause the atoms to merge. At some point, however, the Fermi repulsion becomes equal to the electrostatic attraction and the atoms reach an equilibrium. How far the atoms overlap depends on the strength of the Fermi repulsion, which at equilibrium will be equal, but opposite, to the electrostatic attraction. If the atoms have partially filled valence shells with holes to accommodate the valence electrons of the other atom, an appreciable degree of overlap is possible and in this paper the resulting interaction is called a bond. As the electrostatic attraction in a bond is large, the interatomic distance is short. However, if the outer shells of the atoms are filled, only a small overlap is possible, leading to a much larger separation of the atoms. In this paper such an interaction is called a contact.[2]

When partially filled valence shells overlap, the valence electrons of one atom form electron pairs with those of the other atom. The number of electron pairs (usually non-integral) associated with the bond is a measure of its strength. There are a variety of ways in which this strength can be determined. In the ionic model it is equal to the electrostatic flux linking the two ions, but the flux does not depend on whether the bond is ionic or covalent since it depends only on the number of bonding electrons and not where they reside in the bond (Brown, 2001, p. 30). For equilibrium structures, Preiser *et al.* (1999) showed that the flux associated with a bond is the same as the empirical bond valence which can be calculated from the bond length (§1.2) or, if the structure has no internal strain (§2.4), from the topology of the bond network. The greater the overlap between the atoms, the larger the bond flux or bond valence and hence the greater the attractive force that the bonding electrons exert on their terminal atoms.

Any atom in a structure at equilibrium experiences zero net force acting on it. For a diatomic molecule, the attractive electrostatic force must therefore be exactly equal to the repulsive Fermi force, and since the net force is the derivative of the potential energy, the bonding energy is a minimum (Fig. 1). The distance between the atoms under these conditions is called the *natural length* of the bond or contact. If the bond or contact is stretched by the application of some external force, it exerts a net attractive force pulling its terminal atoms together; if it is compressed, it exerts a repulsive force pushing its terminal atoms apart.

In a solid the situation is more complex. Since each atom forms several bonds, the net force acting on an atom may still be zero even when the bonds individually exert forces. For example, in NaCl the net force acting on each atom is necessarily zero by symmetry even though the Na—Cl bonds may be either all attracting or all repelling their terminal atoms. In this case a second condition is needed to determine the equilibrium bond force, namely, there must be a balance between those bonds and contacts that attract their terminal atoms and those that repel them. If this were not so, the crystal as a whole would contract or expand.

An analysis of the electron density topology in NaCl shows that each Cl atom interacts with its 12 Cl second-neighbours as well as the expected six Na first-neighbours, all 18 atoms being linked by electron density bond paths (Pendás *et al.*, 1998). However, since the valence shells of the Cl atoms are full (after forming bonds with Na), the interactions between Cl atoms are contacts while the interactions between Na and Cl atoms are bonds, each involving 1/6 valence electron pairs. The balance of forces that prevents the equilibrium structure of NaCl from expanding or contracting is therefore a combination of the bond force acting between neighbouring Na and Cl

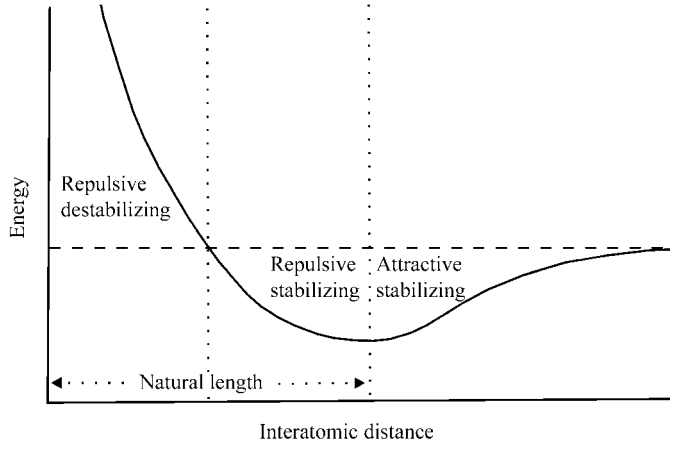

Figure 1
Schematic graph showing the variation of bond energy with interatomic distance for bonds and contacts. The different energy and force regimes are indicated.

[1] In some cases three-body interactions related to the electronic structure of the atom are important, but these cases are not considered here.
[2] The attraction in a contact derives from van der Waals dispersion forces that are not properly modelled using classical electrostatic theory, but since this attraction is much weaker than that in a bond, it is often ignored and does not form part of the quantitative model developed below. The classical model can, therefore, still be used in this analysis.

atoms and the contact force acting between neighbouring Cl atoms. Since the Cl atoms are drawn together by being bonded to a common Na atom, their separation is shorter than their natural length. The contact therefore exerts a net repulsive force on the two Cl atoms. To compensate, the Na—Cl bond must exert an attractive force on the Na and Cl atoms, which means the Na—Cl bond must be longer than its natural length, *i.e.* the Na—Cl bond is stretched.

Both bonds and contacts lower the energy of a crystal, although the binding energy associated with a bond is much greater than that associated with a contact (Dunitz & Gavezzotti, 1999). As shown in Fig. 1, the interaction energy has its largest negative value when the atoms are separated by their natural length. Although small differences from the natural length result in the bond exerting an attractive or repulsive force on its terminal atoms, the binding energy remains negative and changes very little. Only when the bond or contact becomes unphysically short will it be destabilizing, *i.e.* will the binding energy be positive.

1.2. The bond-valence model

Before attempting a quantitative examination of the forces exerted by bonds and contacts, it is useful to review the equations of the bond-valence model which provides the simplest way to determine the number of electron pairs associated with the different bonds and hence the bond lengths. Full details of the model are given in Brown (2001). Discussion of contacts is deferred to the following section since, by definition, they are not associated with bonding electron pairs.

In the ionic limit, Gauss' theorem requires that the sum of the fluxes (*i.e.* bond valences), S_{ij}, received by atom i from the bonds it forms with its ligands, j, be equal to its formal ionic charge, V_i, that is the number of valence electrons the atom uses in bonding. This is expressed by the valence-sum rule

$$V_i = \sum_j S_{ij}, \tag{1}$$

the summation being made over all the bonds formed by the atom. In addition, the flux is distributed between the bonds according to the principle of maximum symmetry which states that a system in equilibrium will have the highest symmetry allowed by the constraints [such as (1)] acting on it. This condition is expressed by the equal valence rule as shown in the Appendix of Brown (1992) as

$$0 = \sum_{\text{loop}} S_{ij}, \tag{2}$$

where the summation, having regard to the direction of the flux, is performed around any closed loop in the bond network.

Equations (1) and (2), which are equivalent to the Kirchhoff equations used to solve electric networks, can be solved for the bond network to give a unique flux for each bond. From this bond flux the length of the bond, R_{ij}, can be calculated using the empirical expression

$$R_{ij} = R_0 - B \ln(S_{ij}), \tag{3}$$

where R_0 and B are constants that are fitted to observed bond lengths under the constraint that (1) is obeyed. Values of these constants, which depend only on the nature of the terminal atoms, can be found in Brown & Altermatt (1985), Brese & O'Keeffe (1991) and Brown (2002). Equations (1) and (2) can be used to determine the flux associated with each bond, while (3) is related to the Fermi repulsion that determines how close, for a given bond flux, the atoms can approach each other.

There are a number of important consequences of these three equations.

(i) It is possible to predict the length of each bond in a crystal provided that we know which atoms are bonded and provided there are no internal strains such as may be caused by the steric effects described in §2.4.

(ii) Although the equations are based on a localized bond model, they take into account the long-range Coulomb interactions, since any change in the flux (valence) of one bond causes a relaxation of the fluxes of all the other bonds in the structure. The reason the localized bond model works is that at equilibrium the atoms adopt an arrangement in which the first neighbours screen out the influence of more distant neighbours.

(iii) The natural length of a bond depends on its flux (valence). A bond with a large flux has a shorter natural length than a bond with a small flux. The bond flux in turn depends on the formal ionic charges and the coordination numbers, not only of its terminal atoms, but also of its more distant neighbours. Making any change in the structure results in a redistribution of the bond flux, producing a change in the length of, and force exerted by, all of the bonds.

(iv) The empirical nature of (3) automatically compensates for a number of systematic effects including the influence of the contacts between ligands as discussed in §2.2.

1.3. Contacts

While the behaviour of a bond depends on many factors, *e.g.* formal oxidation state and coordination number, which are specific to the particular crystal in which the bond occurs, the behaviour of contacts is much simpler. Owing to the weakness of their attractive force their natural lengths are typically large (> 3 Å). Since their length in a crystal is determined by the lengths of the bonds in their associated coordination spheres, contacts are usually much shorter than their natural length and they therefore exert a repulsion on their terminal atoms. In order to prevent the crystal from expanding under these forces, the bonds must, on average, exert a net attractive force on their terminal atoms. This means that most bonds, although not necessarily all, will be stretched, but whether they exert attractive or repulsive forces, the bonds are usually close to their natural lengths and the forces they exert on their terminal atoms are relatively small. Fig. 1 shows the potential energy of two atoms as a function of their separation. The minimum in the potential energy occurs at the natural length, but the stretching or compression that occurs in

the bonds and contacts found in crystals means that the observed distance will in general be larger or smaller than the natural length, the negative slope of the graph giving the force experienced by the terminal atoms.

2. Theory

The quantitative model of the force exerted by a bond on its terminal atoms, introduced in this section, is used to calculate the bond force constant and the bond compressibility.

2.1. Forces acting in bonds

As described qualitatively in §1, the attractive force in a bond is assumed to arise from the electrostatic attraction of the bondong electrons on two terminal atoms. The repulsive force is assumed to be the Fermi force arising from the overlap of the electron densities of the filled shells of the atoms. In this section we develop an expression for the net force exerted by a bond. We use the ionic model, recognizing that the flux is the same for both ionic and covalent bonds (Brown, 2001, p. 30).

There is no simple way of expressing the electrostatic force acting in a bond in terms of the electrostatic flux connecting the two bonded atoms, so, in the spirit of the ionic model, we write the attractive force as the force between two point charges, q,

$$F_a = -k_o q^2/R^2, \tag{4}$$

where $k_o = 1/4\pi\varepsilon_o = 23$ nN Å^2 electrons^{-2} (or 2300 GPa Å^4 electrons^{-2}), R is the bond length in Å, *i.e.* the separation between the ion centers where the point charges representing the ions are assumed to reside, and q is the effective charge carried by the terminal ions. For convenience the modulus of q is used since its sign is included explicitly in the equation, so that each of the items on the right-hand side is positive and the negative sign indicates that F_a, representing a force of attraction acting on the atoms, is negative. The charge, q, is unknown but it is of the order of the electronic charge and is expected to be related in some way to the electrostatic flux of the bond. It is evaluated empirically in §3.2.

There is also no simple theory by which the Fermi force can be derived, but since it is the Fermi force that determines the length of the bond it is reasonable to suppose that it has the same exponential form as that given in (3) with the same softness constant, B. We therefore write the repulsive force in a bond, $F_{\rm rb}$, as

$$F_{\rm rb} = A\exp(-R/B), \tag{5}$$

where A is a (positive) fitted constant, R is the bond length and B is the softness parameter, assumed here following Brown & Altermatt (1985) to be 0.37 (5) Å.

2.2. Forces acting in a coordination polyhedron

In this section we show that the repulsions exerted by the contacts between the ligands in any given coordination polyhedron are automatically included in the bond repulsion term when the repulsion constant A is determined empirically.

Consider the case of an isolated atom, M, surrounded by six atoms, X, to form a regular MX_6 octahedron (Fig. 2). At equilibrium the net force acting on each atom must be zero. This will always be the case for the central M atom because of the symmetric arrangement of the bonds. However, this is not the case for the ligands. The net force acting on a ligand is directed along the bond and has the value

$$0 = F_a + F_{\rm rb} + 4F_{\rm rc}/2^{1/2}, \tag{6}$$

where F_a and $F_{\rm rb}$ are defined by (4) and (5), respectively, and $F_{\rm rc}$ is the net repulsive force exerted by each of the four $X-X$ contacts. As long as $F_{\rm rb}$ and $F_{\rm rc}$ both have the form of (5) and the same value of B, the two repulsive forces can be replaced by a single repulsive force of the same form. Since the constant A is determined using the observed equilibrium distances, R_e, measured around atoms that are already surrounded by ligands, the repulsions exerted by the interligand contacts are automatically included in the determination of A.

Similar arguments apply to other polyhedra and, since B has been determined using bond lengths observed in environments with a variety of coordination numbers, the different coefficients of the $F_{\rm rc}$ term in (6) for different coordination polyhedra are also implicitly taken into account. The contacts that are not taken into account in this analysis are those between atoms that are not part of the same coordination sphere. Where these occur and are important, *e.g.* in quartz, they may result in the crystals being more compressible than would be expected from the bond compressibilities alone.

2.3. Evaluation of *A*

We can evaluate A by setting the net effective force acting in a bond to zero when $R = R_e$, the observed equilibrium bond length for coordinated cations. Although the bonds and contacts under these conditions do exert small forces as discussed in the previous section, we are only interested in the effective force acting on the bond, that is the force adjusted for the effects of anion–anion repulsion. From (4) and (5), therefore,

$$A\exp(-R_e/B) - k_o q^2/R_e^2 = 0, \tag{7}$$

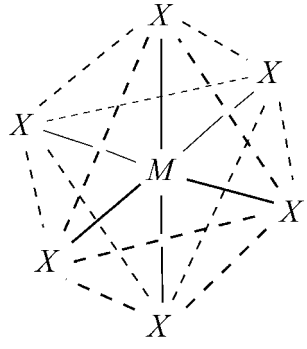

Figure 2
Bonds (solid lines) and contacts (broken lines) in an MX_6 coordination sphere.

where R_e is defined as the *ideal bond length*, *i.e.* the bond length observed in a given coordination polyhedron. It is longer than the natural length because of the anion–anion repulsion, but it is the bond length expected in a crystalline solid in static equilibrium provided that no other constraints[3] are present. In this work we examine how the force exerted by a bond changes when this ideal state is subject to some external constraint such as the application of hydrostatic pressure.

Equation (7) can be rearranged to give an expression for A in terms of R_e,

$$A = k_o q^2/[R_e^2 \exp(-R_e/B)], \tag{8}$$

which can be substituted back into (5) to give the repulsive force,

$$\begin{aligned} F_r &= (k_o q^2/R_e^2) \exp(-(R - R_e)/B) \\ &= (k_o q^2/R_e^2) \exp(-\Delta R)/B), \end{aligned} \tag{9}$$

where $\Delta R = R - R_e$ and F_r, the effective Fermi repulsion, has been written for $F_{\rm rb}$, to indicate that the effects of anion–anion repulsion have been included.

If the bond is strained by some mechanism not considered so far, so that it has a length R, then he bond exerts an effective force F_e on its terminal atoms given by the sum of its (negative) attractive component and its (positive) repulsive component at the new distance, R [*cf.* (7)],

$$F_e = -k_o q^2/R^2 + A \exp(-R/B). \tag{10}$$

Substituting for A from (8) gives

$$F_e = -(k_o q^2/R^2)[1 - (R/R_e)^2 \exp(-\Delta R/B)], \tag{11}$$

which is the effective force exerted by a bond on its two terminal atoms in terms of R, R_e and q. As required, $F_e = 0$ when $R = R_e$.

2.4. What happens when the coordination polyhedron is placed in a crystal?

When the coordination polyhedra are assembled to form a crystal two things may occur. Firstly, since the ligand atoms will bond to other atoms in the crystal, they may no longer be equivalent. Solving (1) and (2) may result in the bonds formed by a given atom having different fluxes and hence different values of R_e and q. Thus, the ideal bond lengths may be changed but F_e would still be zero in the equilibrium structure. Secondly, some bonds may have to be stretched and some compressed in order to make all parts of the structure fit together in three-dimensional space, causing F_e to be different from zero. Such structures are said to be internally strained. It is convenient therefore to divide F_e into two, a force, $F_{\rm int}$, which results from the internal strains, and a force, $F_{\rm ext}$, which results from the application of external constraints, such as temperature or pressure, on the crystal. Either of these forces may result in the bond lengths deviating from their ideal length, R_e. Thus, from (11),

$$F_e = F_{\rm ext} + F_{\rm int} = -(k_o q^2/R^2)[1 - (R/R_e)^2 \exp(-\Delta R/B)]. \tag{12}$$

To simplify the theory, the model is developed on the assumption that $F_{\rm int}$ is zero, which is the case for most of the structures examined. Where $F_{\rm int}$ is not zero, this fact is noted.

In (12) all the quantities on the right-hand side are known except for q, whose evaluation is discussed in §3.2. ΔR is the difference between the actual bond length, R, and the ideal bond length, R_e. If R_e is not known it may be permissible to approximate it in the pre-exponential term by the observed bond length, R, particularly in the limit $\Delta R \rightarrow 0$.

2.5. Bond force constants

The force constant, K, of a bond is given by

$$K = -{\rm d}F_e/{\rm d}R. \tag{13}$$

Consider the case where there are no internal strains ($F_{\rm int} = 0$) so that $F_e = F_{\rm ext}$ and where the displacements from equilibrium are small. K is found by differentiating (12) with respect to R,

$$K = (k_o q^2/R^2)[(1/B)(R/R_e)^2 \exp(-\Delta R/B) - 2/R]. \tag{14}$$

In the limit of small displacements where $R \simeq R_e$, (14) reduces to

$$K = (k_o q^2/R_e^2)(1/B - 2/R_e). \tag{15}$$

However, although (15) may be valid for small changes in the bond length, the exponential term can be approximated by 1.0 only if ΔR is very small. Even when $\Delta R = 0.1$ Å, the exponential term is 0.76, significantly different from 1.0.

2.6. Bond compressibilities

The application of external pressure, P, causes the bond to be shortened resulting in the bond exerting an additional force, $F_{\rm ext}$, on the terminal atoms equal and opposite to the force applied to the bond by the external pressure,

$$P = F_{\rm ext}/gR^2. \tag{16}$$

The term gR^2 is the effective area supported by the bond, g being a geometric factor of the order 1 that represents the ratio of this area to the square of the bond length. Values of g for a number of simple structures are derived in Appendix *A*. The sign in this equation is positive since the application of a positive pressure to the crystal results in the bonds exerting an increased repulsive force on the terminal atoms.

Substituting for $F_{\rm ext}$ from (12) (for $F_{\rm int} = 0$) into (16) gives the pressure as a function of R, R_e and q,

$$P = -(k_o q^2/gR^4)[1 - (R/R_e)2 \exp(-\Delta R/B)], \tag{17}$$

where R is the bond length under pressure and, as before, $\Delta R = R - R_e$.

[3] There are two constraints that can limit the applicability of (7), those resulting from intrinsic electronic anisotropies within the atoms (*e.g.* Jahn–Teller distortions or stereoactive lone pairs) and those caused by steric effects, *i.e.* the constraint that arises when it is impossible to find an arrangement of the atoms in space that allows all the bonds to adopt their ideal lengths, as predicted using (1), (2) and (3) (see §2.4). In such structures some bonds are stretched and some compressed. Except as noted, the discussion in this paper is confined to structures in which these constraints are absent.

Differentiating (17) with respect to R gives

$$dP/dR = -(k_o q^2/gR^4)[(2/R + 1/B)(R/R_e)^2 \times \exp(-\Delta R/B) - 4/R]. \quad (18)$$

In the limit of zero pressure, (18) can be simplified by setting $(R/R_e)^2\exp(-\Delta R/B) = 1.0$,

$$dP/dR = -(k_o q^2/gR_e^4)(1/B - 2/R_e). \quad (19)$$

This approximation is valid for $|\Delta R| < 0.03$ Å, the range typically found at the pressures attained in the laboratory. However, larger compressions are known and if, $\Delta R = -0.1$ Å, the expression on the right hand side of (19) is a factor of two too small.

The bond compressibility, β, is defined as

$$\beta = -(1/R)(dR/dP). \quad (20)$$

Therefore, from (19) and (20) the bond compressibility at zero pressure is

$$\beta = gR_e^3/[k_o q^2(1/B - 2/R_e)]. \quad (21)$$

Hazen & Finger (1979) showed that for many high-symmetry structures in which the bulk compressibility is determined by the compressibility of the bonds,

$$k_b\langle R\rangle^3/s^2 Z_c Z_a \simeq 7.5\,\text{Mbar Å}^3\,\text{electrons}^{-2}, \quad (22)$$

where k_b is the bulk modulus, Z_c and Z_a are the formal cation and anion charges, respectively, and s is an ionicity factor. Hazen & Finger's empirical equation (22) is shown to be approximately equivalent to (21) in Appendix *B*.

3. Comparison with experiment

3.1. Initial test

The above analyses generate two equations, (15) and (21), that can be compared with experiment. The unknown value of q can be eliminated between them to give

$$gR_e/\beta K = 100\,\text{GPa Å}^2\,\text{nN}^{-1}, \quad (23)$$

which contains only experimentally accessible quantities and therefore provides a useful starting point for assessing the validity of the model. The results for a variety of different high-symmetry structures are listed in Table S1,[4] and the average for each structure type, together with its standard deviation, is given in Table 1. The sources of the experimental values of the force constants, K_o, and bond compressibility, β_o, are described in §§3.2 and 3.3, respectively, where the deviations from the theoretical values are discussed. The global average, 114 (σ = 48), is satisfactorily close to the expected value of 100, but the standard deviation is large and the range of individual values runs from a low of 40 for InSb to a high of 237 for LiF. Part of the variation is related to the structure type, particularly for the fluorite, rutile and corundum structures where the ratios are systematically too high, but part of the variation depends on the individual atoms involved, as discussed in the following sections.

Table 1
Test of equation (23) which predicts $gR/(\beta K) = 100$ GPa Å^2 nN^{-1}.

Structure type	Number of structures	$\langle gR/(\beta_o K_o)\rangle$	Standard deviation	Remarks
Fluorite	6	164	20	
CsCl	5	115	21	
NaCl	48	98	48	
Rutile	8	184	20	
Corundum	4	138	15	
Sphalerite	5	107	40	
Wurtzite	7	143	70	122 ± 38 omitting BeO
All compounds	83	114	48	

3.2. Force constants and the evaluation of q

For the high-symmetry compounds used in this study there are not many evaluations of simple bond stretching force constants that can be directly compared with (15), because the bonds are weak and the stretching modes tend to mix with lattice modes and are difficult to isolate. However, Urey–Bradley stretching force constants have been evaluated from IR and Raman spectra for a number of stronger bonds and Brown *et al.* (1997) have shown that there is an approximate relationship between the observed force constant K_o and the bond flux, S (in electrons), given by

$$K_o = aS - [b - \exp(-aS/b)], \quad (24)$$

where a = 450 N m^{-1} electrons^{-1} and b = 140 N m^{-1}. The points shown Fig. 2 of Brown *et al.* (1997) display considerable scatter but the authors were able to define upper and lower limits to this scatter using (24) with a = 505 N m^{-1} electrons^{-1}, b = 100 N m^{-1}, and a = 405 N m^{-1} electrons^{-1}, b = 200 N m^{-1}, respectively. In general, the upper limit gave better predictions for the force constants of bonds between small hard ions, while the lower limit worked better for large soft ions. Since the bond fluxes, S, are readily determined for the high-symmetry structures by assuming that all the bonds are equivalent, a set of 'observed' stretching force constants was calculated using (24).

In (15) all the values on the right-hand side are known except for q. One might expect q to be the same as the formal charge that would be used in a Madelung summation over the whole structure. However, in this model part of the atomic charge is used to shield the bond from the bulk of the crystal so that the effective charge is reduced. Thus q will be less than the formal ionic charge, V, but might be expected to be related to the bond flux, S. Since the form that q^2 takes cannot be determined theoretically, we propose the function

$$q^2 = (8S/3)^{3/2}, \quad (25)$$

designed to give a satisfactory fit between the calculated force constants, K, and the 'observed' force constants, K_o, as noted below. With this function, the values of q range from 0.54 electrons for S = 0.167 to 1.54 electrons for S = 0.667, as shown

[4] Supplementary data for this paper are available from the IUCr electronic archives (Reference: SN0031). Services for accessing these data are described at the back of the journal.

Table 2
Comparison of the theoretical, K, and observed, K_o, force constants.

Structure type	Coordination number	Number of structures	$\langle K/K_o \rangle$	Remarks
Fluorite	8	6	1.05	
CsCl	8	5	0.75	Mostly soft atoms
NaCl	6	48	0.90	
Rutile	6	8	1.39	Mostly hard atoms
Corundum	6	4	1.36	Mostly hard atoms
Wurtzite	4	5	1.19	1.10 with corrected BeO
Sphalerite	4	7	0.94	
All structures		83	0.99	(σ = 0.28)

in Fig. 3. In the unphysical limit of $V < 0.1$, $q \simeq V$, consistent with the notion that the screening provided by the ligands becomes more important the larger the bond flux. It must be emphasized that there is no physical justification for (25) and that other expressions can be found that give almost as good a fit.

The values of K and K_o for individual bonds in the sample of 83 high-symmetry structures are given in Table S1 and their ratios, K/K_o, averaged over all structures belonging to the same structure type, are shown in Table 2. While the global average is close to the expected value of 1 (a consequence of the fitting of q^2), there is significant variation, most of which can be attributed to the approximate nature of (24) and hence to the systematic errors in the value of K_o. For example, (24) predicts that all alkali halides have the same value of K_o (1.69 nN Å^{-1}) since they all have the same bond flux. However, the values calculated using (15) range from 2.88 nN Å^{-1} for LiF to 1.10 nN Å^{-1} for RbI. For small hard ions, the correct value of K_o should be close to the upper limit, calculated from (24) to be 2.73 nN Å^{-1}, which is close to the value of 2.88 nN Å^{-1} predicted by (15) and (25) for LiF.

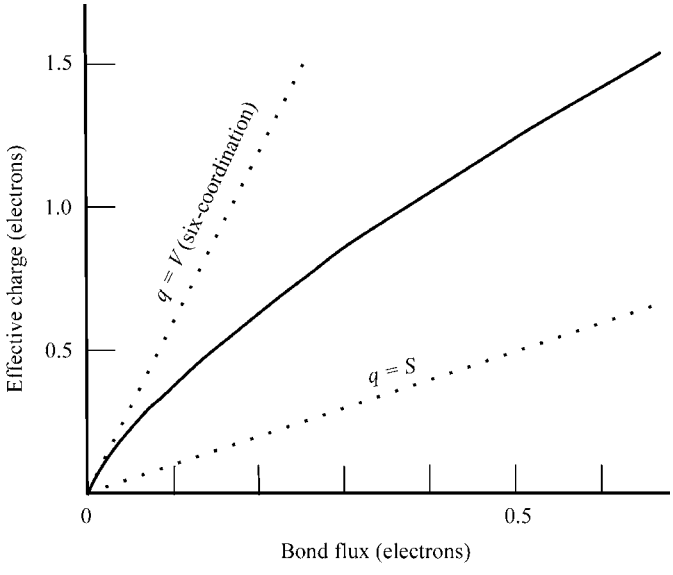

Figure 3
The effective charge, q, in electrons as a function of bond flux, S, calculated according to (25). The broken lines represent the extremes of $q = V$ (for six-coordination) and $q = S$.

Similarly, for large soft ions the value of K_o should be near the lower limit of 1.03 nN Å^{-1}, close to the value of 1.10 nN Å^{-1} predicted by (15) and (25) for RbI. Much of the variation in the values of K/K_o can thus be ascribed to the uncertainties in the value assumed for K_o. Unfortunately, the parameters derived for (24) do not allow a quantitative correction to be made for this systematic effect.

The high ratio found for the wurtzite structures is mostly attributable to the large value of K given by (15) and (25) for BeO (17.0 nN Å^{-1}) compared with the value of 11.3 nN Å^{-1} for K_o given by (24). However, as before, the maximum value of K_o (16.0 nN Å^{-1}) would be more appropriate and this gives good agreement. Substituting this value brings the average ratio for the wurtzite structures acceptably close to 1.0.

Three other structure types in Table 2 have average K/K_o ratios which deviate significantly from 1.0. As indicated in the remarks in the table, this deviation can be attributed to the sample containing either mostly hard atoms, leading to ratios that could be as large as 1.6, or soft atoms, leading to ratios that could be as low as 0.6. Since all the discrepancies can be attributed to the systematic errors in the assumed 'observed' values K_o, (15) and (25) are expected to give a better prediction of the stretching force constant than the empirical correlation of (24).

3.3. Bond compressibility in high-symmetry structures

The bond compressibility is given by (21), where q^2 is assumed to have the value $(8S/3)^{3/2}$ proposed in the previous section.

Values of the compressibilities of 83 different high-symmetry structures are given in Table S1. The experimental values, β_o, are derived from the polyhedral bulk moduli compiled by Hazen & Finger (1979) from crystal bulk moduli drawn from a variety of sources. Most are accurate to around 5%, although a few are considerably less accurate, as noted. In calculating the bond compressibilities we have assumed a uniform contraction of all parts of the structure even when, for example in the case of the corundum structures, the bonds do not contract equally (see §3.4). The average ratios of the bond compressibilities, β, calculated from (21), to the observed bond compressibilites, β_o, are summarized by structure type in Table 3.

The values of the average ratios β/β_o all lie within experimental uncertainty of 1.0, except for the eight-coordinated structures fluorite and CsCl, where the theory gives values that are systematically 50% larger than the observed value, not only for the averages shown in Table 3, but for each of the compounds individually. The reason for this discrepancy is not clear, but it would be removed if the energy of compression were absorbed by 12 bonds per cation rather than the eight that are actually present (see Appendix A). The large value of $gR_e/(\beta_o K_o)$ for fluorite in Table 1 can be attributed to this discrepancy, but for the CsCl structures the large value β/β_o is combined with the low value of K/K_o to give a value of $gR_e/(\beta_o K_o)$ in Table 1 that is close to the expected value.

Within each structure type some systematic variation can be seen. For example, the alkali halides show β/β_o ratios of 1.33, 1.20, 1.15 and 1.12 for F, Cl, Br and I, respectively, but no systematic variation with the cation. A possible reason for this lies in the assumption that all bonds have $B = 0.37$ Å, the value which Brown & Altermatt (1985) determined from observed bond lengths mostly in oxides using (1) and (3). However, B cannot be determined very precisely and Brown & Altermatt (1985) found that any value between 0.32 and 0.42 Å would give a satisfactory fit for most bonds to oxygen. The agreement between the observed and calculated bond compressibilities of the alkali halides would be considerably improved if B were equal to 0.30, 0.32, 0.33 and 0.335 Å for fluorides, chlorides, bromides and iodides, respectively.

The other notable misfits are CuCl and AgI with the sphalerite structure where, surprisingly, the bonds are much less compressible than the model predicts, an effect that is likely to be the result of the different character of the bonds in these compounds.

3.4. Compressibilities of individual bonds

The bond compression can be calculated in more complex structures assuming the pressure is applied uniformly to all bonds. In this case (19) can be written

$$\Delta R = -gR_e^4/[k_o q^2(1/B - 2/R_e)] \cdot \Delta P \qquad (26)$$

This equation holds in the limit of zero pressure, which is adequate for most bonds given the experimental uncertainties in the measured bond lengths. In the case of complex structures, g should have a different value for every bond, but since there is no obvious way to calculate g, a value of 1 is assumed. While values of g different from 1.0 may be the reason why some bond compressions differ from the predicted values, there are usually more plausible explanations which are discussed below. If $(8S/3)^{3/2}$ is substituted for q^2, as in the previous examples, then the expression multiplying ΔP contains only R_e and known constants.

Table 3
Comparison of theoretical, β, and observed, β_o, bond compressibilities.

The standard uncertainty (s.u.) in β_o is around 5% unless otherwise stated.

Structure type	Coordination number	Number of compounds	g	$\langle\beta/\beta_o\rangle$	Remarks
Fluorite	8	6	1.15	1.56	See text
CsCl	8	5	0.58	1.54	See text
NaCl	6	48	1.00	1.04	
Rutile	6	8	1.53	1.00	
Corundum	6	4	1.38	1.17	s.u. ∼15%
Sphalerite	4	5	2.31	1.14	0.95 omitting CuCl, AgI
Wurtzite	4	7	2.31	1.16	s.u. ∼15%
All structures		83		1.12	s.u. ∼15%

Table 4
Observed and predicted [see (26)] bond strains over the applied pressure range.

ΔR(obs) is the difference between the shortest and longest reported bond lengths. Owing to experimental uncertainties, these are not necessarily the bond lengths reported at the highest and lowest pressures.

Bond	R_{eq} (Å)	S	$-\Delta R(\text{obs})^+$ (Å)	$-\Delta R$(pred) (Å)
BeO	(ICSD-62726)	Pressure range 5.0 GPa		
Be—O	1.646	0.49	0.012 (2)	0.007
Be—O	1.655	0.48	0.013 (5)	0.008
Al_2O_3	(ICSD-9770)	Pressure range 4.6 GPa		
Al—O	1.856	0.53	0.010 (2)	0.009
Al—O	1.971	0.39	0.004 (2)	0.017†
$FeTiO_3$	(ICSD-30670)	Pressure range 4.61 GPa		
Fe—O	2.078	0.39	0.026 (2)	0.020
Fe—O	2.201	0.28	0.025 (2)	0.040†
Ti—O	1.874	0.85	0.005 (2)	0.004
Ti—O	2.087	0.48	0.015 (2)	0.015
SiO_2 quartz	(ICSD-100341)	Pressure range 6.14 GPa		
Si—O	1.605	1.05	0.005 (3)	0.003
Si—O	1.614	1.03	0.005 (3)	0.003
$CaMg(CO_3)_2$	(ICSD-66333)	Pressure range 4.69 GPa		
Ca—O	2.381	0.34	0.042 (2)	0.044
Mg—O	2.081	0.35	0.025 (3)	0.024
C—O	1.287	1.24	0.004 (3)	0.001
Ni_2SiO_4	(ICSD-200129)	Pressure range 3.82 GPa		
Ni—O	2.061	0.33	0.020 (3)	0.021
Si—O	1.657	0.91	0.004 (3)	0.002
$Mg_3Al_2(SiO_4)_3$	(ICSD-200341)	Pressure range 4.0 GPa		
Mg—O	2.188	0.26	0.032 (4)	0.038
Mg—O	2.341	0.17	0.034 (4)	0.090†
Al—O	1.875	0.50	0.012 (5)	0.008
Si—O	1.626	0.99	0.007 (4)	0.002
$ZrSiO_4$	(ICSD-100239)	Pressure range 4.83 GPa		
Zr—O	2.127	0.58	0.013 (2)	0.010
Zr—O	2.270	0.40	0.007 (2)	0.022†
Si—O	1.616	1.02	0.005 (2)	0.002

† The calculated compression differs by more than 3σ from the observed strain.

The maximum strains observed and calculated for a variety of bonds in different low-symmetry compounds are given in Table 4. In each case the pressure range is also given and further details can be found in Table S2.

The predicted compressions for bonds with valences larger than 0.7 lie within the limits of experimental uncertainty, therefore, only the weaker bonds can usefully be compared with experiment. For most of the compounds, agreement between the calculated and observed values of ΔR is satisfactory. The reasons for the exceptions, marked with a dagger, are discussed below.

3.4.1. BeO. This compound provides a chance to compare the predictions of Table 3 with those of Table 4 by recognizing that ΔR is proportional to β. The values of ΔR calculated using (26) are ∼50% lower than the observed values, but the compressibility calculated using (21) (0.0020 GPa^{-1}) is ∼50% higher than that determined from the bulk modulus [0.0013 (3) GPa^{-1}]. The discrepancy is attributable to the different values of g used in (21)

(2.31) and (26) (1.00). However, the differences between the observed and predicted values of ΔR are not significant at the 3σ level.

3.4.2. Al_2O_3. This structure illustrates the problems associated with calculations based on a model in which all bonds are assumed to show equal compressive strain. Two Al atoms are brought close together across a face shared between two AlO_6 octahedra. The repulsion between the Al atoms causes each of them to be displaced from the center of its octahedron, giving three short and three long Al—O bonds. The compression of the long Al—O bond is restricted by the need to simultaneously compress the short Al—Al contact. The compression of the short bond is predicted correctly by (26), but the long bond is much less compressible than predicted. In spite of the failure of the equal strain assumption, the compressibility calculated using (21) (0.0016 GPa^{-1}) is the same as the experimental compressibility derived from the bulk modulus [0.0014 (2) GPa^{-1}].

3.4.3. $FeTiO_3$. Ilmenite has an ordered arrangement of the corundum structure with short Fe—Ti contacts across the shared octahedral face. As the bonds are longer, the repulsion between the cations is not as large as in the case of Al_2O_3, but, even so, the weaker Fe—O bonds to the shared face do not contract as much as predicted by (26).

3.4.4. $Mg_3Al_2(SiO_4)_3$. The garnet pyrope is an example of a structure in which the bonds show internal strain ($F_{\rm int}$ not equal to zero). The Mg atom is eight-coordinate and occupies a cavity that is too large (the Mg—O bonds are stretched). The assumptions made in deriving (26) tend to overestimate the expected compression and the high symmetry of this structure prevents the two bonds from compressing independently.

3.4.5. $ZrSiO_4$: zircon. As in the case of garnet, the eight-coordinate Zr forms four long and four short bonds with the compression of the ZrO_8 coordination sphere constrained by the shorter (least compressible) of the two bonds.

3.5. Calculation of bond valences in structures under pressure

In addition to providing information on the strain produced in a bond under pressure, (26) also provides a method of correcting the bond-valence parameter R_0 used in (3) to calculate bond valences, when the bond length has been measured under pressure. Since the parameter R_0 is the notional length of a bond of unit valence, it is only necessary to replace R_e in (26) by R_0 and S by 1.0. As before, in the absence of any better information, g is set to 1.0 giving the relatively simple expression for dR_0/dP shown below, (27),

$$dR_0/dP = 10^{-4}R_0^4/(1/B - 2/R_0)\ \text{Å}\ GPa^{-1}. \qquad (27)$$

4. Conclusions

In this paper we have explored the forces that are exerted between neighbouring atoms in the localized bond model of a compound. Brown *et al.* (1997) have previously shown that this model can be used to relate the thermal expansion of bonds to the bond force constant and hence to the bond flux. This paper extends this work by showing that the bond force constant itself can be derived from a simple physical model of the bond and that the model also accounts for the compressibility of bonds subject to hydrostatic pressure. As the earlier study showed, the bond properties, such as thermal expansion or compressibility, are not independent of the structure in which they appear. To the extent that they depend on the bond flux, they depend on the way in which the atoms are linked to form the bond network, but they are also affected by steric constraints which may limit the strain a particular bond can display. The simple equations derived in §2 provide a first estimate of the force constant and compressibility of a given bond, but the observed compressibility requires that the steric constraints also be taken into account.

The bond force model presented here offers the possibility of exploring the internal strains as well as dynamical aspects of a crystal using an intuitive localized bond model, its simplicity providing insights that more complex models cannot. Such analyses are beyond the scope of the present study whose purpose is to present the model and demonstrate how well it works in accounting for two straightforward force-related properties.

APPENDIX *A*
Determination of *g*

A1. Derivation of *g*

The geometric factor, g, is calculated by considering that the work done in compressing a crystal is used entirely to compress the bonds. It is assumed that the atoms in the high-symmetry binary compounds have ideally symmetric coordination with all bonds having the same length, R. It is also assumed that compression reduces all bonds uniformly and that the bond angles do not change; g is then evaluated at zero pressure, but the difference is small over the pressure ranges accessible to measurement.

The work done in compressing the crystal is

$$P\ dV = NF\ dR, \qquad (28)$$

where P is the pressure, V the volume of the unit cell, N the number of bonds in the unit cell and F the force required to compress the bond whose length is R.

The volume of the cell (except for triclinic cells) is given by

$$V = abc\ \sin\gamma \qquad (29)$$

where a, b, c and γ are cell constants (assuming a unique c axis).

These are related to the bond length, R, by

$$\begin{aligned} a &= AR \\ b &= BR \\ c &= CR, \end{aligned} \qquad (30)$$

where A, B and C are geometric constants that depend on the structure.

Therefore

$$V = ABC \sin\gamma R^3 \tag{31}$$

and

$$\mathrm{d}V = 3ABC \sin\gamma R^2 \mathrm{d}R. \tag{32}$$

Substituting into (28)

$$3ABC \sin\gamma PR^2 \ \mathrm{d}R = NF \ \mathrm{d}R$$
$$F = (3ABC \sin\gamma R^2/N)P. \tag{33}$$

Recognizing that $F = -F_{\rm ext}$ in (16),

$$g = 3ABC \sin\gamma/N \tag{34}$$

A2. Evaluation of *g*

Structure	*ABC*	*N*	*g*	
Fluorite	$A = B = C = 4/3^{1/2}$ $\sin\gamma = 1$	32	1.15	
CsCl	$A = B = C = 2/3^{1/2}$ $\sin\gamma = 1$	8	0.58	
NaCl	$A = B = C = 2$ $\sin\gamma = 1$	24	1.00	
Rutile	$A = B = (2^{1/2} + 1)$ 1 $C = 2^{1/2}$ $\sin\gamma = 1$	6	1.54	Cation–cation distance included in *N*
Corundum	$A = B = 6^{1/2}$ $C = 4(3^{1/2})$ $\sin\gamma = 0.866$	78	1.38	Cation–cation distance included in *N*
Sphalerite	$A = B = C = 4(3^{1/2})$ $\sin\gamma = 1$	16	2.31	
Wurtzite	$A = B = (8/3)^{1/2}$ $C = 8/3$ $\sin\gamma = 0.866$	8	2.31	

APPENDIX *B*
Reconciliation with the equation of Hazen & Finger

Hazen & Finger (1979) showed that the empirical formula (35) gives a good fit to experiment.

$$k_b R^3/(s^2 Z_c Z_a) = 7.5\ \mathrm{MBar\ \AA^{-3}}, \tag{35}$$

where k_b is the bulk modulus, s an ionicity factor and Z_a the anion charge. The bulk modulus is related to the linear (bond) compressibility by (36)

$$k_b = 1/(3\beta) \tag{36}$$

so that (35) can be rewritten as

$$\beta = R^3/(2250 s^2 Z_c Z_a)\ \mathrm{GPa^{-1}}, \tag{37}$$

where the distances are given in Å and the charges in electrons.

Noting that the value of $s^2 Z_a$ is approximately 0.8 (range 0.75–1.0) using the values of s given by Hazen & Finger (1979), (37) reduces to

$$\beta = R^3/(1800 Z_c)\ \mathrm{GPa^{-1}}, \tag{38}$$

which can be compared with (21),

$$\beta = gR^3/[k_o q^2 (1/B - 2/R)]. \tag{39}$$

Noting that $(1/B - 2/R)$ has a value of approximately 1.7 $\mathrm{\AA^{-1}}$, setting $g = 1$ and substituting for k_o [see (4)] gives

$$\beta = R^3/(3910 q^2)\ \mathrm{GPa^{-1}}. \tag{40}$$

Eliminating β between (38) and (40) gives

$$q^2/Z_c = 0.46,$$

in satisfactory agreement with values ranging from 0.46 to 0.52 for $Z_c > 1$ (0.25 for $Z_c = 1$) using q^2 calculated from (25) for the structures listed in Table S1.

We would like to thank R. T. Downs and M. Kunz for reviewing an early draft of this paper. This work was supported by a research grant from the National Research Council of Canada.

References

Bader, R. F. W. (1990). *Atoms in Molecules, International Series on Monographs in Chemistry 22*. Oxford University Press.
Brese, N. E. & O'Keeffe, M. (1991). *Acta Cryst.* B**47**, 192–197.
Brown, I. D. (1992). *Z. Kristallogr.* **199**, 255–272.
Brown, I. D. (2001). *The Chemical Bond in Inorganic Chemistry*. Oxford University Press.
Brown, I. D. (2002). *Accumulated list of bond valence parameters*, http://ccp14.ac.uk/ccp/web-mirrors/i_d_brown.
Brown, I. D. & Altermatt, D. (1985). *Acta Cryst.* B**41**, 244–247.
Brown, I. D., Dabkowski, A. & McCleary, A. (1997). *Acta Cryst.* B**53**, 750–761.
Dunitz, J. D. & Gavezzotti A. (1999). *Acc. Chem. Res.* **32**, 677–684.
Hazen, R. M. & Finger, L. W. (1979). *J. Geophys. Res.* **84**, 6723–6728.
Pendás, A. M., Costales, A. & Luaña, V. (1998). *J. Phys. Chem. B*, **102**, 6937–6948.
Preiser, C., Lösel, J., Brown, I. D., Kunz, M. & Skowron, A. (1999). *Acta Cryst.* B**55**, 698–711.